

The Mechanism of Xuanyu Tongjing Decoction Regulating NOD/NF κ B Pathway to Inhibit Ectopic Tissue Inflammation to Reduce Ovarian Damage in Rats with Ovarian Endometriosis

Weisen Fan¹, Fengting Zhai², Zheng Yuan², Guotao Hu¹, Li Wang²

¹Department of Gynecology, Guang'anmen Hospital, China Academy of Chinese Medical Sciences, Beijing, 100053, People's Republic of China;

²Department of Gynecology, Affiliated Hospital of Shandong University of Traditional Chinese Medicine, Jinan, 250013, People's Republic of China

Correspondence: Fengting Zhai, Email zft0326@163.com

Introduction: In traditional Chinese medicine texts, Xuanyu Tongjing Decoction (XYTJD) is a prescribed remedy for premenstrual belly pain and dysmenorrhea. It is currently routinely used to treat ovarian endometriosis (OEM) with good outcomes.

Aim: In order to investigate the underlying processes of Xuanyu Tongjing Decoction in treating OEM inflammation and reducing ovarian damage.

Methods: We created a rat model of OEM and carried out transcriptome sequencing. Batch molecular docking technique in conjunction with Ultra-high-performance liquid chromatography-quadrupole-time-of-flight-high-resolution mass spectrometry was used to screen the main active components in Xuanyu Tongjing Decoction.

Results: The ectopic cyst was firmly attached to the ovary in our successfully created rat model of ovarian endometriosis. According to GSEA enrichment study, XYTJD may up-regulate pathways linked to oocyte formation in ovarian tissues and down-regulate immunological and inflammatory pathways in ectopic tissues. Rat ectopic tissues and human ectopic tissues showed a similar pattern in the expression of the NOD/NF κ B pathway during the proliferative phase. In ectopic tissues of rats, XYTJD may down-regulate the NOD/NF κ B pathway and suppress the expression of TNF- α and IL-1 β , which are downstream inflammatory factors in this pathway. In addition, XYTJD may restore the down-regulation of cAMP/PI3K/AKT and lower the expression of apoptotic factor CASP9, endoplasmic reticulum stress protein SEC61B and antioxidant protein GSTM5 in the ovary with ectopic tissue attachment. Following identification, the three samples' intersection included 10 active compounds in total. There was a 21-component overlap in active ingredients between rat and human serum. After a preliminary virtual screening, β -Hederin, Proanthocyanidin A2, and Cimicifida E were suggested to be the essential components that interfere with NOD/NF κ B.

Conclusion: In rats with proliferative OEM, XYTJD may down-regulate the NOD/NF κ B pathway in ectopic tissues, consequently alleviating ovarian tissue damage by reducing inflammation brought on by ectopic tissues.

Keywords: ovarian endometriosis, inflammation, ovarian damage, pharmacology of traditional Chinese medicine

Introduction

In obstetrics and gynaecology, ovarian endometriosis(OEM) is a frequent benign cyst illness. In addition to causing dysmenorrhea, OEM might harm ovarian reserve, which can interfere with a patient's ability to get pregnant usually.¹ When the OEM steadily swells in size, it will burst and generate pelvic adhesions, leading to chronic pelvic pain in patients. Furthermore, OEM has a specific cancer rate.² Surgical treatment can eliminate the cyst, but illness recurrence remains a problem. Although hormone-suppressive medicines can alleviate symptoms and lower the size of cysts in the treatment of OEM, they will still recur after drug withdrawal, accompanied by numerous adverse effects.³ OEM symptoms can cause patients to experience anxiety and sadness, which is not conducive to everyday work.⁴ As a result, OEM continues to be a challenging issue in scientific and clinical research.

OEM is a type of chronic inflammatory disease in which inflammation not only causes dysmenorrhea, pelvic adhesions, and persistent pelvic discomfort but also damages the ovarian function of the cyst attachment, resulting in infertility.^{5,6} OEM typically produces proinflammatory factors such as TNF- α and IL-1 β . TNF- α Increased TNF- α levels in ovarian follicles after ectopic tissue attachment can promote the NF κ B pathway in granulosa cells and inhibit telomerase activity, hindering follicle growth.⁷ According to Fonseca's research, ovarian follicular fluid from OEM patients with ectopic tissue attachment had considerably higher levels of IL- β and IL-18 expression, suggesting that ectopic tissue attachment is a factor in ovarian inflammation.⁸ Persistent ovarian inflammation can cause tissue fibrosis and ovarian oxidative stress, which can impact follicle formation.⁹ When used to treat endometriosis, traditional Chinese medicine provides the benefits of modest side effects and a stable curative effect. It also reduces dysmenorrhea, improves pregnancy, and prevents recurrence. Prior clinical research has demonstrated^{10,11} that Xuanyu Tongjing Decoction (XYTJD) can dramatically reduce the symptoms of dysmenorrhea, mitigate the damage to ovarian function following OEM, and suppress serum levels of matrix metalloproteinase-9 and endometrial antibodies. Therefore, in this study, we established unilateral ovarian endometriosis rats using the most recent ovarian endometriosis modelling method, conducted a thorough transcriptome analysis to fully understand the mechanism of XYTJD in treating OEM inflammation and mitigating ovarian damage, and screened the active ingredients in XYTJD to inhibit inflammation.

Materials and Methods

Experimental Reagents

Estradiol benzoate (Shanghai Quanyu Biotechnology Animal Pharmaceutical: 240337), sesame oil (Shanghai Yuanye Biotechnology: BYBZ23929), sodium penicillin (Shandong Bomi Biotechnology: QMS-50) (1.6 \times 10⁵U·kg⁻¹ penicillin sodium), crystal violet solution (Biosharp: BL802A), cell culture medium (Beijing Soleobal: 240006015), HE staining solution (Servicebio: G1005-100ML), NOD1 Rabbit pAb (Abclonal: A1246), NOD2 Rabbit pAb (Abclonal: A25228), RIPK2 Polyclonal antibody (Proteintech: 15366-1-AP), Anti-I κ B gamma Rabbit pAb (Servicebio: GB11628-100), Anti-I κ B alpha Rabbit pAb (Servicebio: GB111509-100), NF κ B1 Polyclonal antibody (Proteintech: 14220-1-AP), Anti-IL-1 beta Rabbit pAb (Servicebio: GB11113-100), Anti-TNF-alpha Rabbit pAb (Servicebio: GB11188-100), Anti-ADCY2 Rabbit pAb (Servicebio: GB114825-100), PDE3B Polyclonal antibody (Proteintech: 25290-1-AP), Anti-AKT3 Rabbit pAb (Servicebio: GB115583-100), Anti-PI3 Kinase p85 alpha Rabbit pAb (Servicebio: GB11525-50), GSTM5 Polyclonal antibody (Proteintech: 14502-1-AP), Anti-GSTM5 Rabbit pAb (Servicebio: GB113591-100), SEC61B Polyclonal antibody (Proteintech: 25290-1-AP), Caspase 9 Polyclonal antibody (Proteintech: 25290-1-AP).

Instrument

Freezing microtome (Thermo Fisher Scientific: CRYOSTAR NX50), Gel imaging system (Alpha Corporation: 2200), Electrophoresis instrument (Thermo: EC250-90, USA); Bell pendulum decolorization shaker (Sevier Biotech: DS-2S100), Vortex mixer (Xavier Biotech: MV-100), Handheld centrifuge (Xavier Biotech: D1008E), Ultra-high liquid chromatograph (ACQUITY UPLC H-Class, Waters, USA), High-resolution mass spectrometer (Xevo G2-XS QTOF MS, Waters, USA:).

OEM Animal Model

Vital River Laboratory Animal Technology provided the 45 female SD rats (9 weeks old) used in this study. Staining and observation of vaginal smears lasted for ten days. After determining that each rat had a regular oestrous cycle, 45 rats were randomly split into groups A, B, and C. Estradiol benzoate and sesame oil were combined in a 1:3 ratio to create a mixed solution. Six rats from group C were chosen at random as donor rats. The recipient groups were groups A and B. Before being transplanted, the donor rats received two intraperitoneal injections of an estradiol benzoate combination at 100 μ g/Kg once every four days. Routine preparation was completed before surgery, and isoflurane was utilized during surgery to maintain anaesthesia in recipient rats at a dosage of 2%. Following cutting and trimming into 1cm \times 2mm long strips, the donor rats' uteri were submerged in cell culture media. One rat's lateral abdomen was chosen, and an incision parallel to the rat's spine measuring approximately 1.5 cm was made. Toothed forceps were used carefully to remove the fat surrounding the rat's ovary.

The ovary was then fixed, and a fine-tipped forceps (ST-15) was used to insert the ectopic tissue into the fat at the base of the ovary until it broke through. The ovary was subsequently pushed into the abdominal cavity and sutured layer by layer.

To avoid infection, penicillin sodium (8U/d) was intraperitoneally given to each donor for three days following the operation. Donor rats received 200µg/kg estradiol benzoate solution intraperitoneally every four days for two consecutive injections. On the eighth day after surgery, two rats were randomly chosen from the recipient group for laparotomy. The appearance of ectopic tissue cysts in the ovary's periphery and endometrial stroma and glands, as detected by HE staining, demonstrated the model's effectiveness. Group A was unilateral OEM + XYTJD gavage, Group B was unilateral OEM + normal saline, and Group C was normal rats + normal saline. Intragastric administration began on the seventh day following surgery and lasted for two weeks. To cover the rats' oestrous cycle, 100µg/Kg of estradiol benzoate was given subcutaneously into the necks one week before sampling. Following the removal of ectopic, ovarian, and uterine tissues under isoflurane anaesthesia, the rats in each group were sacrificed via carotid artery exsanguination.

Transcriptome Sequencing

The Trizol magnetic beads method extracted total RNA from ovarian, ectopic, and uterine tissue. NanoDrop 2000 identified the concentration and purity of the RNA, while Agilent 2100 assessed the quality of the nucleic acid. The library building was carried out using the Illumina Truseq™ RNA Sample Prep Kit, and the sequencing platform was the Illumina NovaSeq 6000. After collecting raw sequencing data (raw reads), clean reads with Q20>85% and Q30>80% were filtered. The clean reads from all samples were assembled de novo using Trinity, and the initial assembled sequences were optimized and filtered using TransRate¹² and CD-HIT.¹³ The integrity of the transcriptome was assessed using BUSCO.¹⁴ Gene expression was calculated using RSEM,¹⁵ whereas transcripts per million¹⁶ were used to compute each group's gene and transcript expression. DESeq2¹⁷ was used to examine the differences in expression between several groups. The screening conditions for differentially expressed genes (DEGs) were set to $|\log_2FC| \geq 1$ and $P \leq 0.05$.

UPLC-Q-TOF-HRMS

The composition of XYTJD is as follows: fried radix paeoniae alba 30g, wine anglicae sinensis radix 30g, Moutan Cortex 30g, fried gardenia 18g, fried semen sinapis 12g, radix bupleuri 6g, Rhizoma Cyperi 6g, vinegar curcuma radix 6g, wine radix scutellariae 6g, glycyrrhizae radix 6g. Shandong Xinzonglu Traditional Chinese Medicine Hospital supplies traditional Chinese medicine through its pharmacy department. The conventional Chinese medication was submerged in 500mL pure water for an hour before boiling and extracting the liquid. The medication solution was stored for 15 minutes after the initial boiling. Continue to add 300mL of water, cook for 10 minutes, decant the second solution, and combine the two. Finally, the two drug solutions were concentrated to a volume of 400mL, with a drug concentration of 0.375g/mL. The gavage dose was 1mL/mouse each day. Serum samples were taken seven days following the gavage. In group A, blood samples were obtained from the orbit after 30 minutes, 45 minutes, and 60 minutes of gavage for serum detection. Following an ethical assessment, OEM patients were recruited and given an informed consent form. Informed consent was obtained from the patients prior to the initiation of the study. On an empty stomach, 200mL of XYTJD was given, and venous blood was extracted after 30, 60, and 90 minutes. Ultra-high-performance liquid chromatography-quadrupole-time-of-flight-high-resolution mass spectrometry (UPLC-Q-TOF-HRMS) was utilized for detection after the resultant blood was allowed to stand and centrifuged to extract serum.

Liquid phase:¹⁸ Liquid mobile phase: waters BEH C18 column (1.7µm, 2.1*50mm); Mobile phase: A: 0.1% formic acid; B: 0.1% formic acid acetonitrile; Gradient elution: (0–2min, 95%A, 5%B; 2–30min, 95%–2%A, 5%–98%B; 30–35 min, 2%A, 98%B; 35–39 min, 2%–95% A, 98%–5% B; 39–40min, 95%A, 5%B); Flow rate: 0.4mL/min column temperature: 40°C; The detection volume was 3µL. The detection conditions of the positive mode of mass spectrometry were as follows: nitrogen flow rate 800L/h; Voltage 2kv; Desolvation temperature 400°C; The ion source temperature was 110°C. Collision voltage 20–40V; The collection mass number ranged from 50 to 1200. The detection condition of the negative electric mode of mass spectrometry was 1.5kv, and the other setting conditions were the same as those of the positive electric mode.

Acquisition of Differently Expressed Genes in Human Ectopic Tissues

Using the R language, the sequencing data of normal female endometrial tissue in the proliferative phase and ectopic human endometriosis tissue were obtained from the GEO database (<https://www.ncbi.nlm.nih.gov/>). The limma package was used for between-sample batch effect processing to perform differential expression analysis of the two types of tissues after gene IDs in the data were translated to gene names. The criteria for differentially expressed genes were $|\log_2FC| \geq 1$ and $P < 0.05$. For the bioinformatics study, the differentially expressed genes between endometriosis and normal uterine tissues (DEGsEN) were discovered, and the results were compared with sequencing data from an OEM rat model.

Data Analysis

The whole workflow of UNIFI¹⁹ natural goods, together with the entire TCM database, was utilized to process the data of the three samples. Venny was used to take the intersection of the active ingredient data from the three samples. The ingredients that finally intersected were normalized using the PubChem website, and the chemical structure was queried. The UniProt database was utilized to find relevant targets, while the PDB database was used to identify essential target structures. The active compounds were docked to the key targets using computer virtual screening, and the key active components were initially screened based on their molecular binding energy, which ranged from small to big.

Following the acquisition of DEGsAB, DEGsBC, and DEGsEN, the intersection genes of the three sets of DEGs were identified using Venny2.1.0. The expression of intersection genes was then displayed in each group of rats using a volcano plot. GEGsAB and DEGsEN were enriched using KEGG pathways, and the resulting pathways were shown using bubbles and bar graphs. The immune infiltration was analyzed using Cibersort, and the differences in immune cell infiltration across the rat groups were displayed using box plots. GSEA was used to examine pathway changes in ectopic tissues of AvsB and BvsC; the intersection pathways of GSEA (AvsB) and GSEA (BvsC) were shown by a two-way bar chart; the changes of intersection pathways in GSEA (EvsN) were noted; and a GSEA trend chart showed the significant pathways. The GSEA pathway alterations in each group's ovarian tissues were illustrated using the same methodology. The network was plotted after using miRWalk to query miRNAs regulating essential targets.

WB

Total protein was extracted from ectopic, ovarian, and uterine tissues, and the protein concentration was calculated. After boiling to cool, the proteins were separated by electrophoresis, transferred to PVDF membranes, and blocked at room temperature for 15 hours. At 4°C, primary antibodies were incubated for the entire night in a refrigerator. After hatching the secondary antibody for two hours at room temperature, the bands were exposed to the gel imaging system. ImageJ software analysed The protein grey value, and an appropriate internal control was selected based on the molecular size of the protein as control.

HE Staining and Immunohistochemistry

Using liquid nitrogen, ovarian, ectopic, and uterine tissues were quickly frozen. A small amount of freezing section embedding agent was added after the freezing microtome had returned to room temperature, and the temperature was regulated before the section was fixed. Under a microscope, the histomorphological alterations of the ovaries and ectopic tissues were observed using HE staining following fixation.

Frozen pieces were dried at room temperature, baked, and fixed with methanol. After washing, an antigen repair solution was used to inhibit endogenous peroxidase for antigen repair. After serum blocking, primary antibodies were stored in the refrigerator and incubated overnight at 4 °C. The next day, secondary antibodies were incubated at room temperature for 50 minutes. DAB chromogenic solution was applied, then counterstained with hematoxylin for roughly 3 minutes before reverting to blue with hematoxylin reverting solution and waBshing under running water. After dehydration and sealing, the slides were examined using a white light microscope.

Results

The Therapeutic Component in XYTJD

After identification, 97 active components were found in XYTJD liquid using UPLC-Q-TOF-HRMS, 30 in human drug-containing serum, and 29 in rat drug-containing serum. There were 21 active components in the serum of both rats and humans. Table 1 and Figure 1 depict these 21 active components' structures. The mass spectra of the three samples are displayed in Figure 1a–f.

Table 1 Detailed information of the 21 active ingredients in UPLC-Q-TOF-HRMS

NO	Component name	Molecular formula	m/z	Time
1	3-O-Benzoyl-20-deoxyingenol	C27H32O5	437.2345; 437.2340; 437.2346	10.14(a);10.17(c);10.14(e)
2	21 α -hydroxy-3-oxo-oleane-11,13(18)-diene-28-acid	C30H44O4	469.3279; 469.3274; 469.3297	25.88(a);35.89(c);35.89(e)
3	23-Acetyl Alismaketone A	C32H50O6	531.3672; 531.3675	31.81(a);31.79(c)
4	25(S)-Ruscogenin-1-O- β -D-xylopyranosyl-(1 \rightarrow 3)- β -D-fucopyranoside	C38H60O12	709.4165; 709.4171	31.00(e);31.00(c)
5	beta-Hederin	C41H66O11	735.4628; 735.4635	30.97(e);30.98(c)
6	Bisabolone-9-one	C15H22O2	235.1686; 235.1678; 235.1683; 235.1670	23.73(c);29.02(c);29.19(c);29.19(e)
7	Blestrianol D	C29H24O5	453.1662; 453.1663; 453.1668	24.99(c);25.15(c);25.15(e)
8	Calcium oxalate	C2CaO4	128.9506; 128.9507; 128.9508; 128.9502;	0.6(a);1.51(c);4.02(e);39.40(e)
9	Cimisine E	C35H54O8	603.3866; 603.3853	31.10(c);31.09(e)
10	Delbrusine	C27H43NO7	494.3113; 494.3133	31.91(c);31.92(e)
11	Esculentagenin	C31H46O8	547.332; 547.3317	11.46(c);11.44(e)
12	Ethyl Linoleate	C20H36O2	309.2785; 309.2783	31.79(c);31.79(e)
13	Ginsenoside RG2	C42H72O13	785.5002; 785.4968;785.5015	31.96(c);31.16(e);31.96(e)
14	Hellebrigenin	C24H30O6	415.2106; 415.2105; 415.2104	24.99(a);25.15(c);25.15(e)
15	Lucidenic acid A	C27H38O6	459.2777; 459.2780	10.65(c);10.63(e)
16	Mulberrofuran A	C25H28O4	393.2085;393.2083;393.2073;393.2083	9.62(a);9.62(c);9.59(e);38.85(e)
17	Oleanolic acid beta-D-glucopyranosyl ester	C36H58O8	619.4215; 619.4192	31.69(c);31.68(e)
18	Picfeltaerinen X	C36H56O11	665.3901; 665.3880	31.04(c);31.04(e)
19	Proanthocyanidin A2	C30H24O12	577.1339; 577.1329	28.81(c);28.81(e)
20	Schizonepetoside E	C16H28O8	349.1831; 349.1824	38.84(c);38.84(e)
21	Trilinolein	C57H98O6	879.7404; 879.7407	38.82(c);38.83(e)

OEM Rat Model

During modelling, no recipient rats passed away. During feeding, no rats perished. Following gavage, the rats were dissected, and it was discovered that 11 rats in group B and 13 in group A had ovarian cysts. A characteristic of the effective rat model was developing a tight connection between endometriotic cysts surrounding the ovary. Figure 2a-c display the model's details. The ectopic tissue is strongly connected to the ovary, as demonstrated by HE staining. Estrogen caused ectopic tissue to develop noticeable cysts, and the cyst wall revealed noticeable endometrial stromal cells and glands. The uterine tissue of a normal rat with a normal arrangement of stromal and epithelial cells is displayed in Figure 2d and e.

Transcription Analysis of Ectopic Tissues

By evaluating the intersection, ten active components were discovered to occur in all three samples. For details, see Figure 3a. Five ectopic tissues were picked from groups A and B, whereas three normal tissues were chosen from group C. Following ectopic tissue and normal tissue sequencing analysis, 1098 DEGsAB were obtained between groups A and B, and 4605

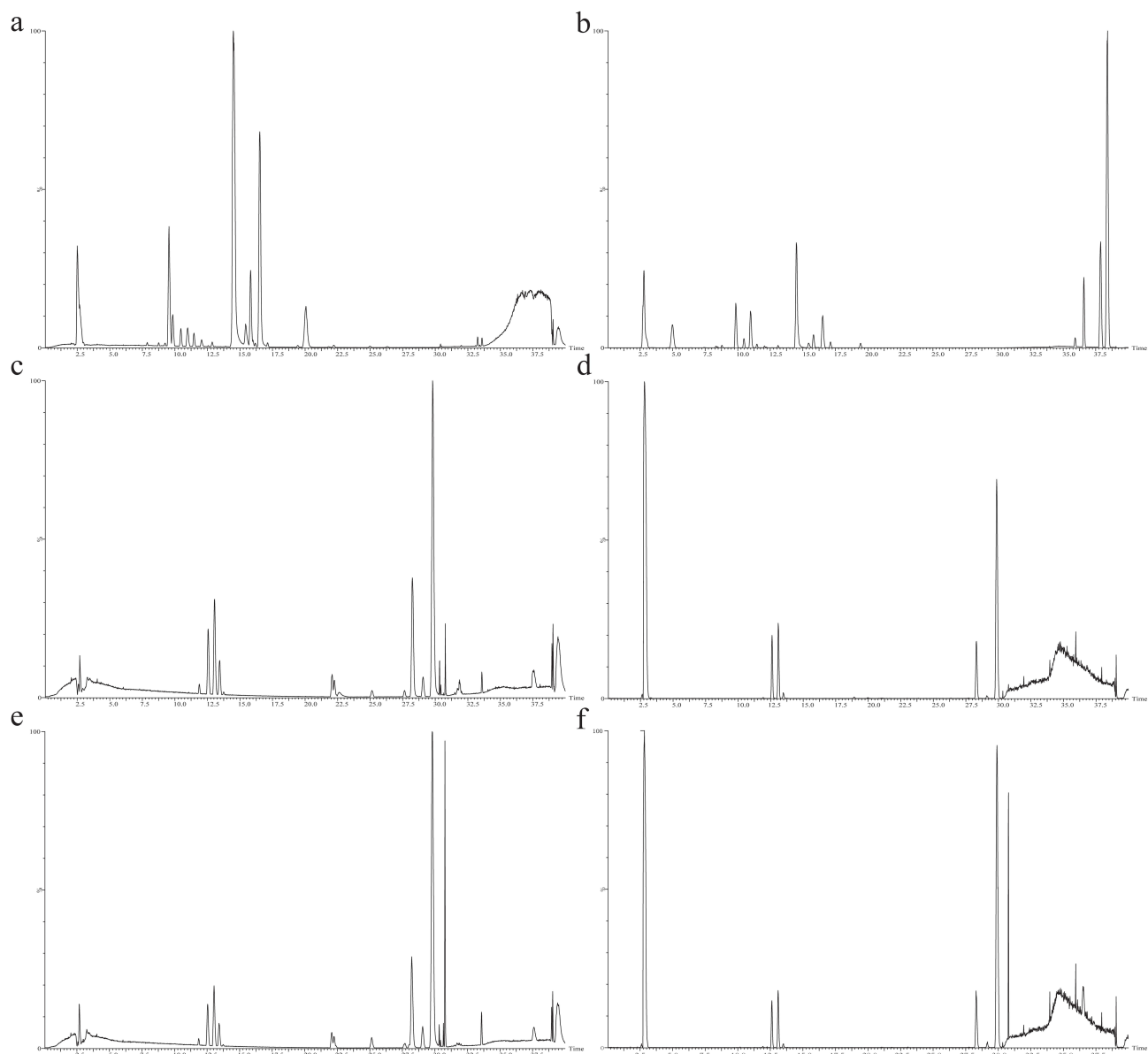


Figure 1 Continued.

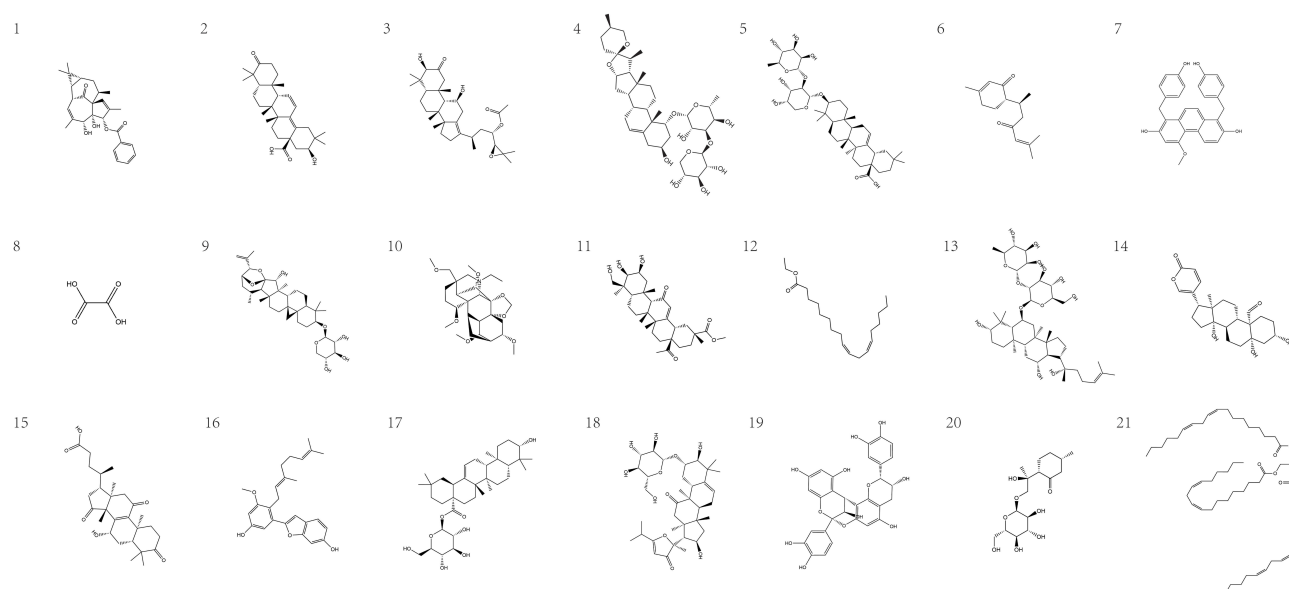


Figure 1 Shows the three samples' mass spectra and 21 molecular structures. (a) XTTJD's mass spectrum in the positive electric mode; (b) XTTJD's mass spectrum in the negative electric mode; (c) positive charge mode mass spectra of human drug-containing serum; (d) negative charge mode mass spectra of human drug-containing serum; (e) positive charge mode mass spectra of rat drug-containing serum; (f) negative charge mode mass spectra of rat drug-containing serum. 1–21 are the 21 active component structures that intersected in both human and rat drug-containing serum. 1.3-O-Benzoyl-20-deoxyingenol; 2.21 α -hydroxy-3-oxo-olean-11,13(18)-diene-28-acid; 3.23-Acetyl Alismaketone A; 4.25(S)-Ruscogenin-1-O- β -D-xylopyranosyl-(1 \rightarrow 3)- β -D-fucopyranoside; 5.beta-Hederin; 6.Bisabolone-9-one; 7.Blestrianol D; 8.Calcium oxalate; 9. Cimicide E; 10.Delbrusine; 11.Esculentagenin; 12.Ethyl Linoleate; 13.Ginsenoside RG2; 14.Hellebrigenin; 15.lucidenic acid A; 16.Mulberrofuran A; 17.Oleanolic acid beta-D-glucopyranosyl ester; 18.Picifetarraenin X; 19.Proanthocyanidin A2; 20.Schizonepetoside E; 21.Trilinolein.

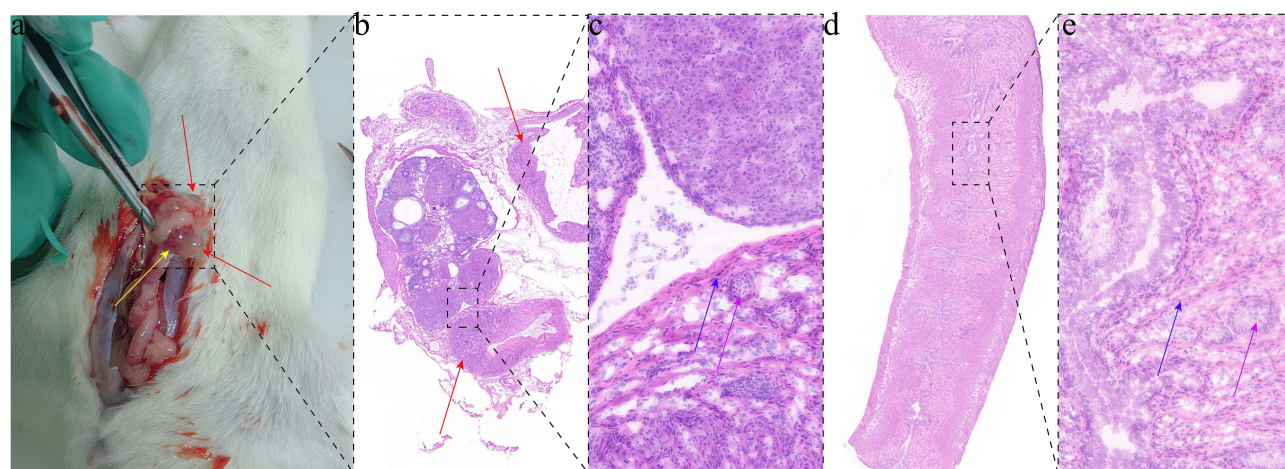


Figure 2 Modeling of Unilateral OEM. (a) Unilateral ovarian endometriosis model anatomy. The red arrows depict endometriotic cysts, while the yellow arrows represent the ovaries. (b) HE staining of unilateral OEM. The red arrow in the illustration depicts an ectopic cyst that is tightly attached to the ovary. (c) Micrograph showing ectopic tissue linking with ovarian tissue; blue arrows represent endometrial stromal cells; purple arrows represent endometrial glands. (d) Normal uterine tissue of rats throughout the proliferative period; (e) microscopic image of the endometrium in uterine tissue, with blue arrows denoting endometrial stromal cells and purple arrows representing endometrial glands.

DEGsBC between groups B and C. Ectopic tissue sequencing data are available in [Supplementary Table 1](#). 365 DEGsEN were obtained by comparing human ectopic tissues with normal tissues. The transcriptome chips used in this comparison were GSE5108, GSE25628, GSE153739, and GSE201912. From the GEO data, 21 ectopic tissues and 10 normal tissues in the proliferative phase were chosen. The 18 DEGs common to the three comparisons were obtained by taking the intersection by Venn diagram. For details, see [Figure 3b](#). The combined volcano plot was used to visualize the expression of 26 DEGs, as shown in [Figure 3c](#). 38 pathways were identified by KEGG enrichment analysis of DEGsAB; they included the TGF- β pathway linked to fibrosis, the PI3K-Akt pathway related to cell proliferation, and the cell adhesion molecules associated to

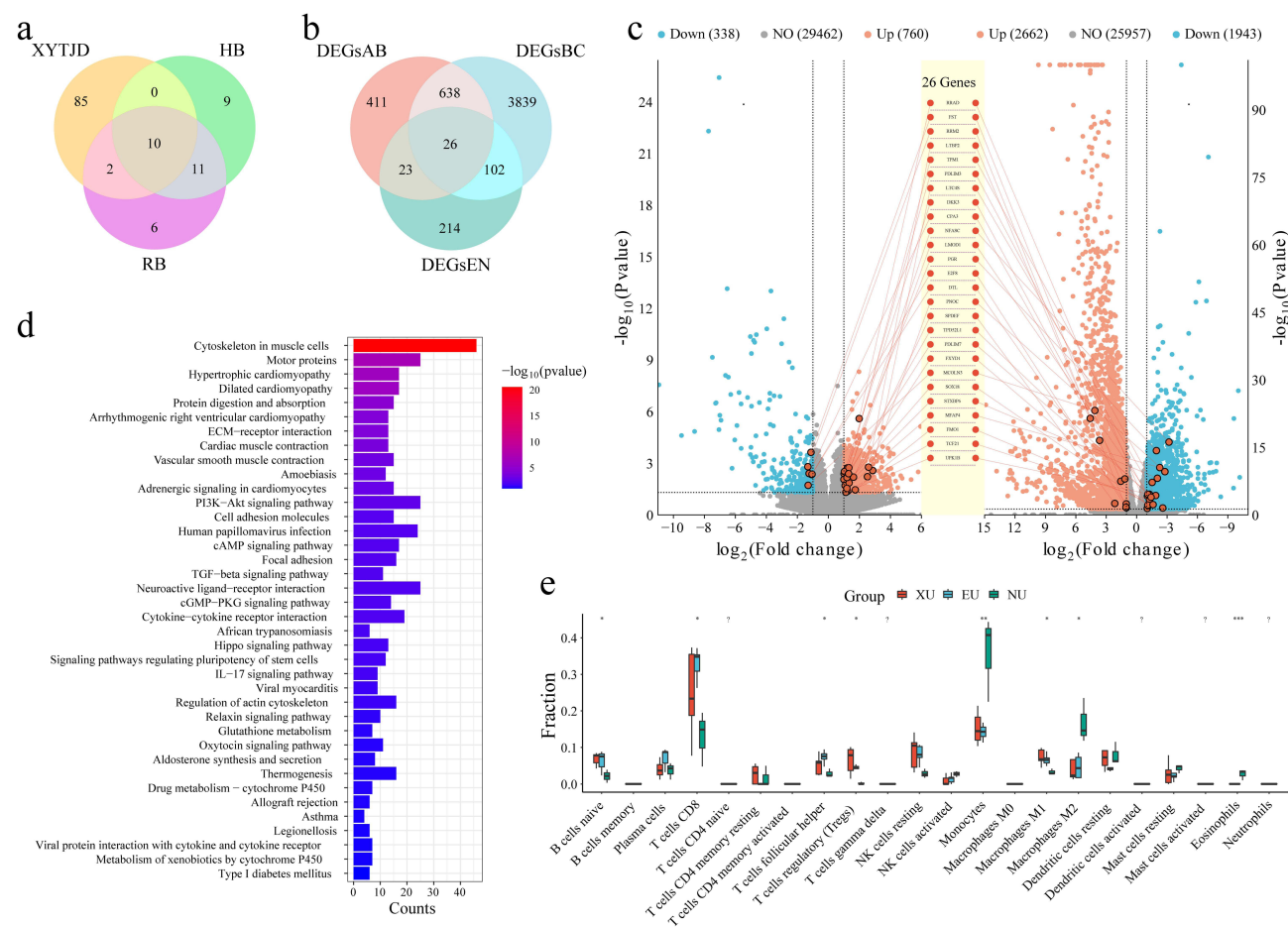


Figure 3 Transcriptome analysis of tissues that are ectopic. (a) Venny diagrams for the three tested items' active ingredients were detected using UPLC-Q-TOF-HRMS. HB represents human blood; RB represents rat blood. (b) Venn diagram depicting the intersection of DEGs in ectopic tissues; (c) Expression of the 18 DEGs at junction in combined AvsB and BvsC volcano plots of ectopic tissues; (d) 38 pathways' KEGG enrichment acquired by DEGsAB; (e) Analysis of the immune infiltration in the ectopic tissues of groups A, B, and C.

cell adhesion. Details are shown in Figure 3d. The ectopic tissues in group B exhibited a decrease in resting dendritic cell clusters and an increase in M1 macrophage, T follicular helper cells, resting natural killer cells, and plasma cell clusters compared to the normal tissues in group C. Figure 3e provides more information.

XYTJD Downregulated the NOD/NF κ B Pathway in Ectopic Tissues During the Proliferative Phase

Groups A, B, and C's ectopic tissues were subjected to GSEA enrichment analysis, which revealed 60 significant pathways in GSEA (AvsB) and 64 in GSEA (BvsC). A two-way bar graph was used to show the expression trend of the 38 pathways obtained through the intersection in AvsB and BvsC. Figure 4 reveals that inflammation pathways, including NF κ B, JAK-STAT, and NOD-like receptors, were elevated in ectopic tissues compared to normal tissues, which XYTJD could down-regulate. The Nod-like receptor pathway is an upstream pathway of the NF κ B pathway. Endometriosis development and progression are linked to the NOD/NF κ B pathway. Figure 4d and e provide further details on how the pathway trend map via GSEA might display changes in essential targets in NOD/NF κ B. It was discovered that the tendencies in NF κ B, JAK-STAT, and natural killer cell-mediated cytotoxicity were similar to those in rats by examining the GSEA enrichment analysis of human ectopic tissues and normal tissues, which displayed 38 pathways at the intersection of rat tissues. Details can be found in Figure 5a. Following DEGsEN enrichment analysis, the human KEGG pathway additionally included the NF κ B pathway. Figure 5b provides more information. By predicting the

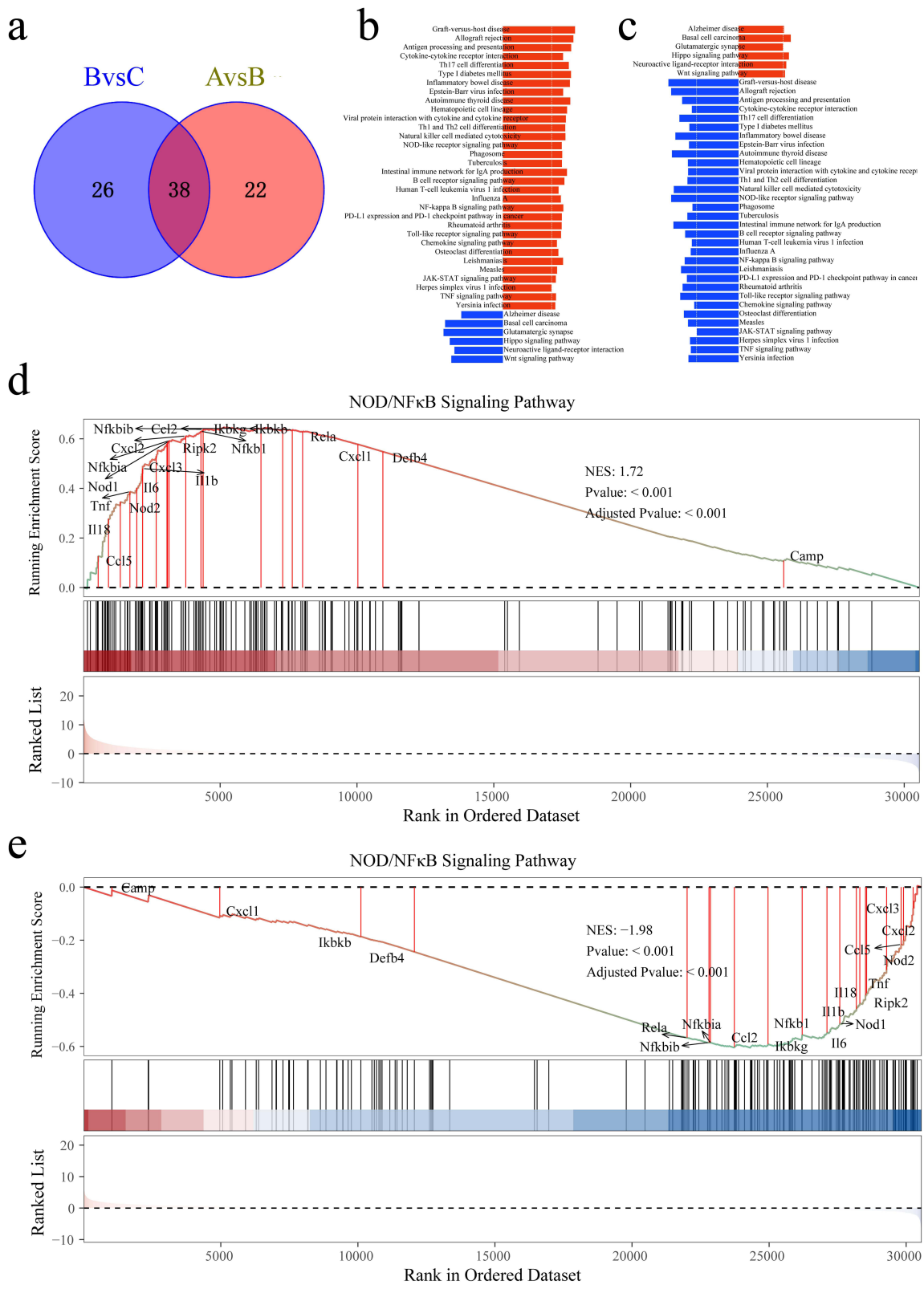
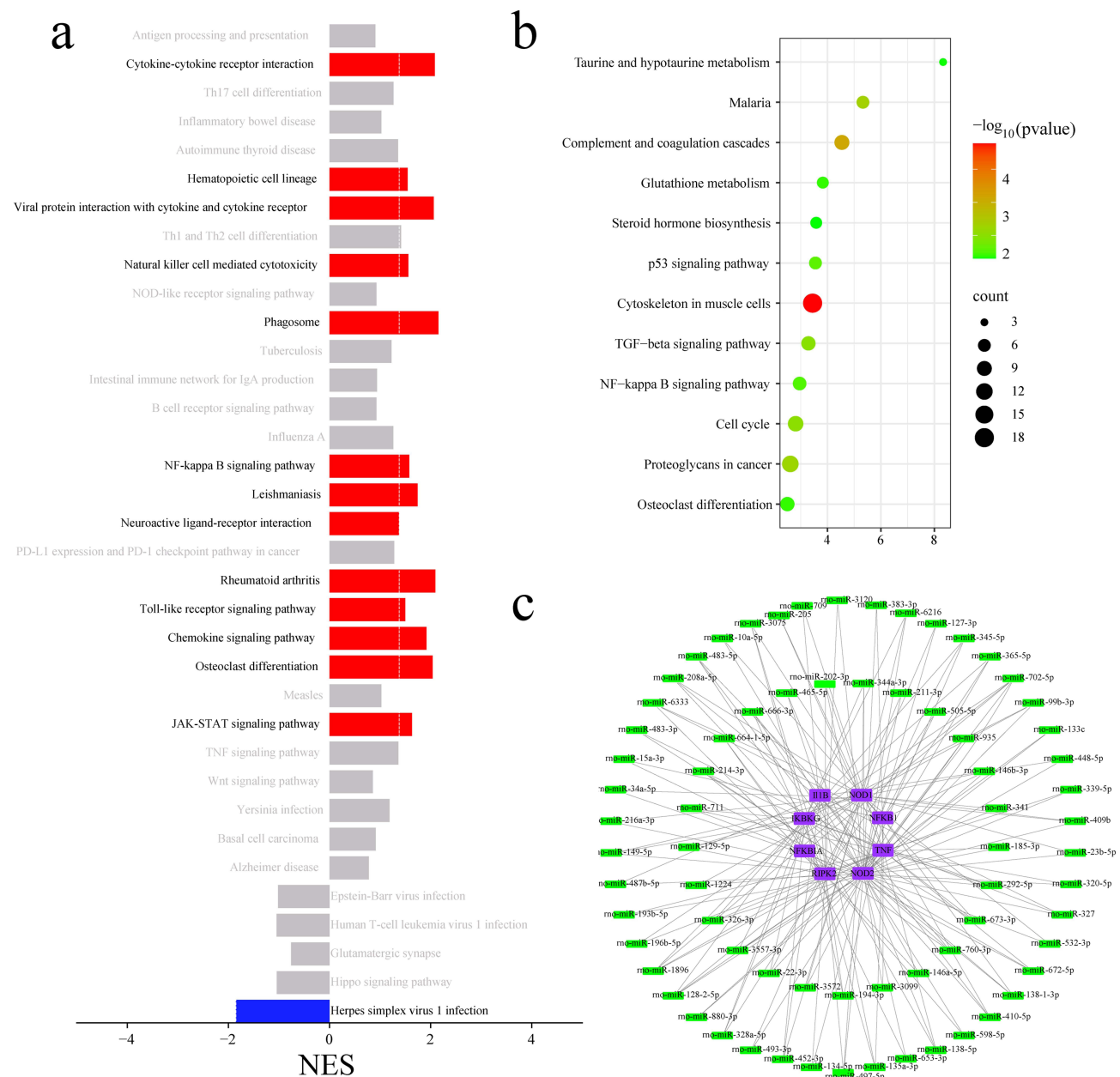


Figure 4 Ectopic tissue GSEA enrichment analysis. (a) Meaningful paths at the intersection of GSEA (AvsB) and GSEA (BvsC); (b) 38 intersecting pathways' expression trend in BvsC; (c) 38 intersecting pathways' expression trend in AvsB; (d) Expression of the NOD/NFκB pathway trend map in BvsC; (e) Expression of the NOD/NFκB pathway trend map in AvsB.

miRNAs that can regulate NOD/NFκB, we can better understand the mechanism of XYTJD, which lays a foundation for our future research. Figure 5c provides more information.

GSEA Enrichment Analysis of Ovarian Tissue

3 normal ovarian tissues were chosen from group C, and 4 ovarian tissues connected to ectopic tissues were selected from groups A, and B. GSEA enrichment study revealed that ovarian tissue had 32 significant GSEA (BvsC) pathways and 55 significant GSEA (AvsB) pathways (Pvalue < 0.05). By intersection, 5 significant GSEA pathways were discovered. The GSEA trend map demonstrated that XYTJD up-regulated the five pathways of intersection, which were down-regulated in the ectopic tissues of group B relative to the normal ovaries of group C. Among them are the PI3K-AKT and cAMP pathways essential for follicular growth. For details, see Figure 6a–c. An upstream pathway of PI3K-AKT is cAMP. The GSEA pathway



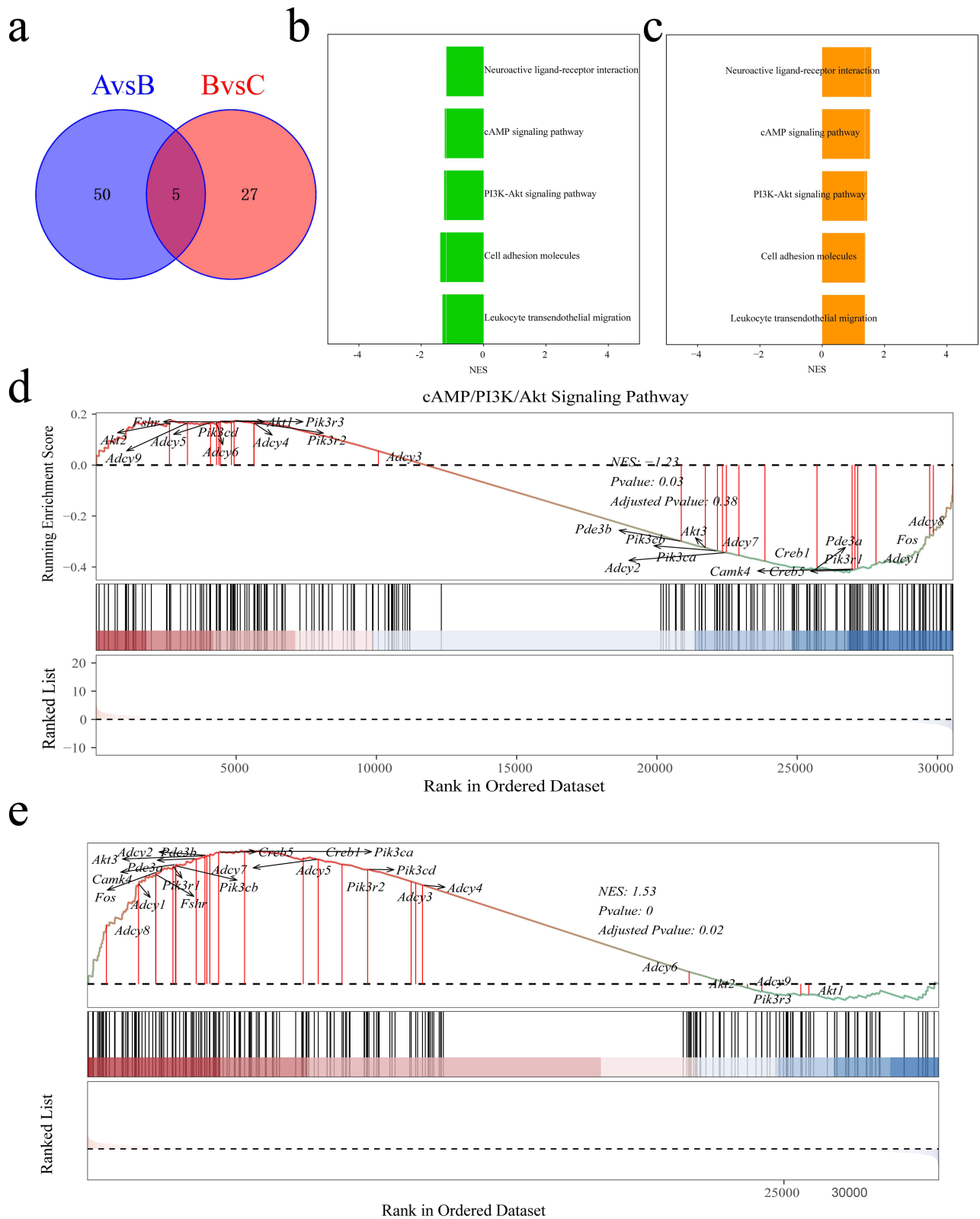


Figure 6 GSEA enrichment analysis of the ovary. (a) GSEA (AvsB) and GSEA (BvsC) enriched pathway intersection plots; (b) 5 intersecting pathways' expression patterns in BvsC; (c) 5 intersecting pathways' expression patterns in AvsB; (d) GSEA expression trend of cAMP/PI3K/AKT in BvsC; (e) GSEA expression trend of cAMP/PI3K/AKT in AvsB.

trend was utilized to illustrate the cAMP/PI3K/AKT variations in the ovarian tissue's AvsB and BvsC. Details are shown in [Figure 6d](#) and [e](#). Ovary tissue sequencing data are available in [Supplementary Table 2](#).

Key Targets and Pathway Validation

In the proliferative phase, XYTJD could down-regulate NOD1, NOD2, RIPK2, IKBKG, NFKBIA, NFKB1, IL-1 β and TNF- α in NOD/NF κ B pathway in ectopic tissues. See [Figure 7a](#) for more information.

During the proliferative phase, the ectopic tissue attached ovary had lower expression of ADCY2, PDE3B, AKT3, and PIK3R1 in the cAMP/PI3K/AKT pathway than the normal rat ovary. After XYTJD treatment, the expression of the aforementioned aberrant targets was restored in ovarian tissues connected to ectopic tissues. CASP9 is a downstream factor of PI3K/AKT that promotes apoptosis. AKT can suppress the expression of CASP9. XYTJD decreased the expression of CASP9 in ovarian tissues with ectopic tissue attachment. Furthermore, ectopic tissue attachment dramatically elevated the expression of antioxidant protein GSTM5 and endoplasmic reticulum channel protein SEC61B in the ovary, which could be reduced by XYTJD intervention. See [Figure 7b](#) for more information. Details of the protein expression bar plot are shown in [Figure 7c-q](#). XYTJD was able to lessen the high expression of SEC61B and GSTM5 in ovarian stroma and follicles, as demonstrated by [Figure 8](#) Immunohistochemistry. As illustrated in [Figure 8](#), immunohistochemistry confirmed that NF κ B1 and IL-1 β displayed the same pattern as WB. [Figure 9](#) explains how XYTJD reduces ovarian damage from ectopic tissue by downregulating the inflammatory pathway NOD/NF κ B.

Virtual Screening

21 active components intersecting in the two species' sera and 18 targets in the NOD/NF κ B pathway were used for batch molecular docking. Active compounds with small target energy were screened based on the total energy needed for batch molecular docking. The ingredients that had lower binding energies were beta-hederin, Cimicide E, Proanthocyanidin A2, and 25(R)-ruscogenin-1-O- β -D-xylopyranose(1 \rightarrow 3)- β -D-fucopyranoside. The data of the computer virtual screening are shown in [Figure 10](#).

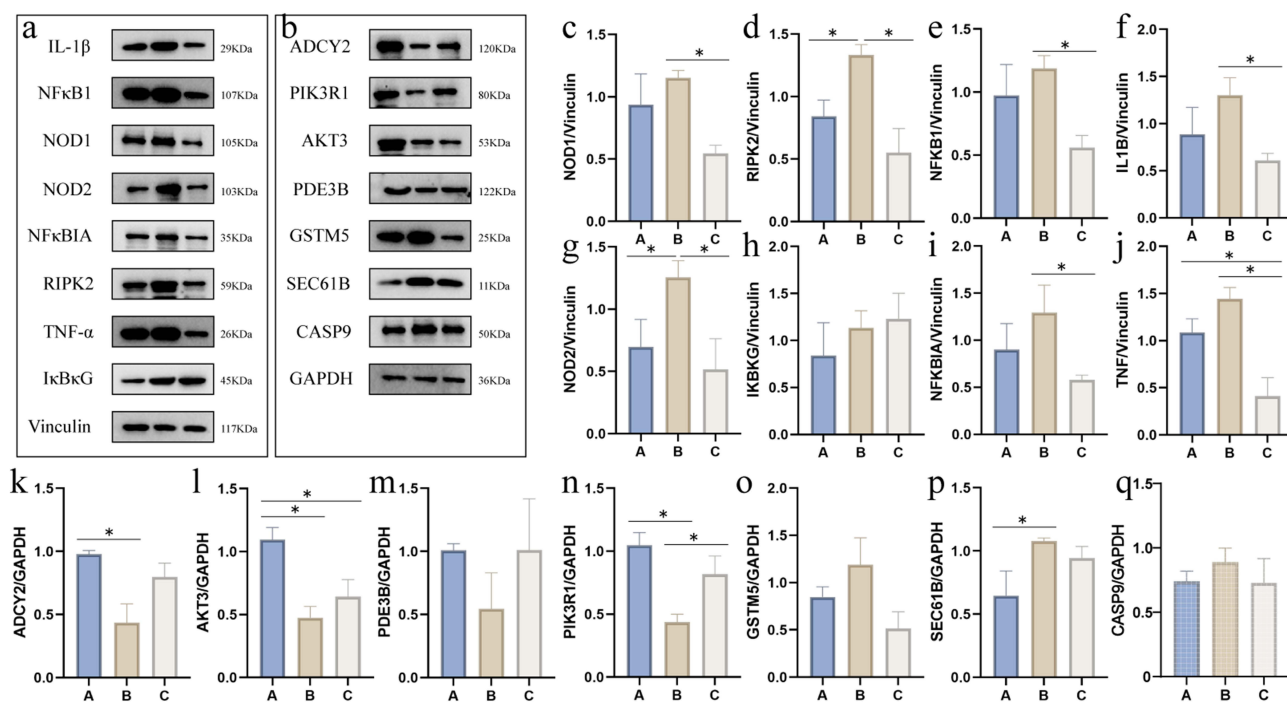


Figure 7 Validation of important targets in ovarian and ectopic tissues. (a) Expression trends of NOD/NF κ B pathway targets in endometriotic tissues; (b) Trends in the expression of CASP9, GSTM5, SEC61B, and cAMP/PI3K/AKT in ovarian tissues; (c–q) Protein expression bar graph. Each group underwent three repetitions of the experiment.

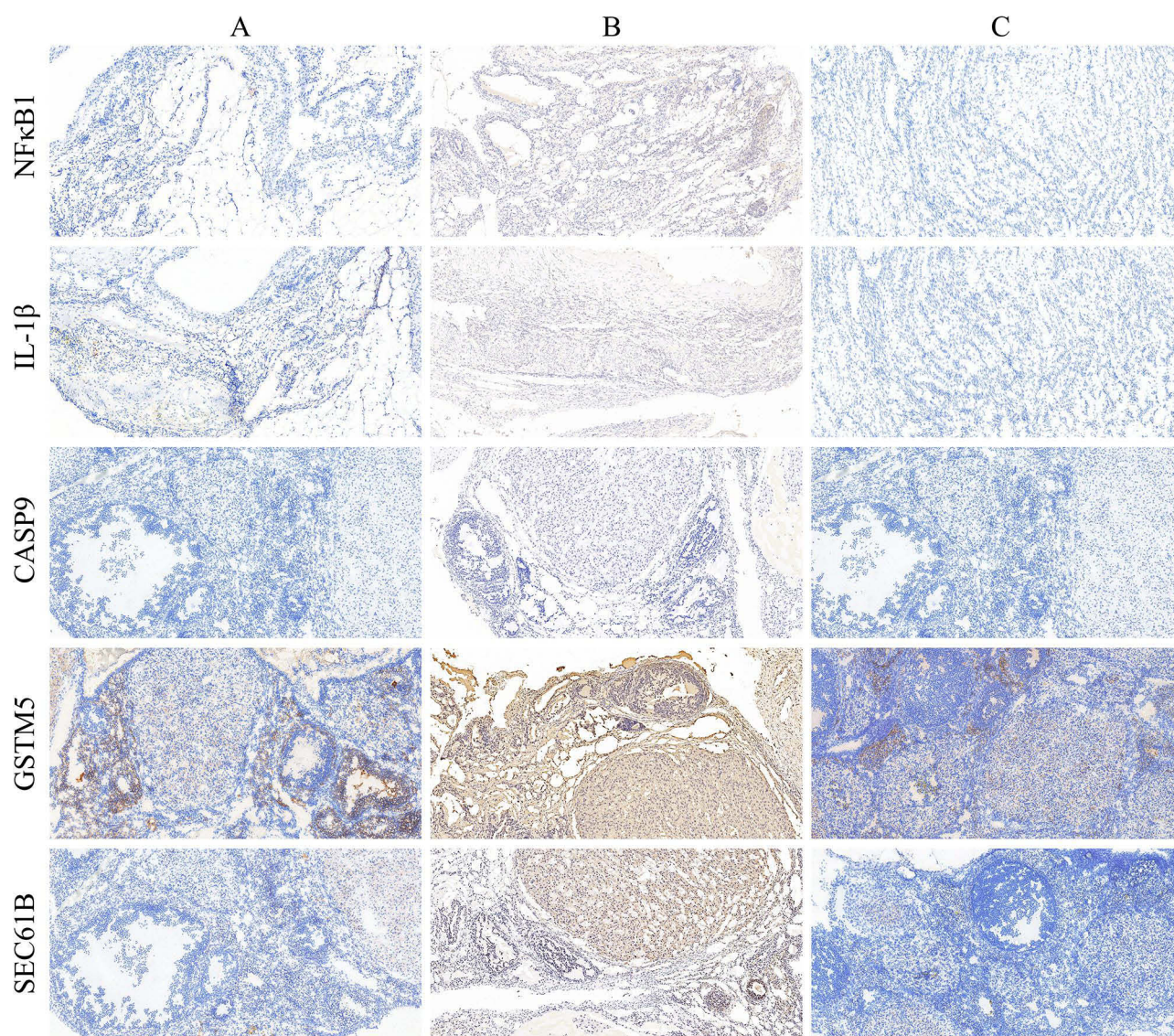


Figure 8 Immunohistochemistry. (A-C) This figure's left side represents the detected target, while its upper side is labeled as the group. In ectopic tissues, the detection targets were NFκB1 and IL-1β, while in ovarian tissues, they were CASP9, GSTM5, and SEC61B. Normal ovarian and endometrial tissue made up Group C. The slices were 10 times larger thanks to the CaseViewer program.

Discussion

When OEM occurs in a person, the ovaries and cysts are closely linked; sometimes, the cysts have even penetrated the healthy ovarian tissue. Surgical removal of the cyst frequently results in the loss of normal ovarian tissue, which compromises ovarian function.²⁰ Even after surgery, there is a significant risk that OEM will recur. Regardless of whether OEM satisfies the surgical requirement or not, it will disrupt reproductive function and cause dysmenorrhea in patients, which is directly associated with periodic bleeding and persistent inflammation of the lesion.⁶ Estrogen released by the ovaries is the mediating factor in chronic inflammation. Thus, to examine the impact of XYTJD on inflammation in ectopic tissues, we engaged ovarian tissues in the proliferative phase and ectopic tissues. Most endometriosis-related animal experiments focus only on ectopic lesions in the mesentery and peritoneum. No research has been done on stopping ectopic tissue from causing damage to ovarian tissue.²¹ To replicate the human OEM as closely as possible, the OEM rat ectopic tissue in this work was closely attached to the ovary, and cysts were developed when estrogen was present.

The intersection of DEGsAB, DEGsBC, and DEGsEN yielded 26 intersection targets. By presenting the expression trend of intersecting targets in AvsB and BvsC using a combined volcano diagram, it was discovered that ectopic tissues

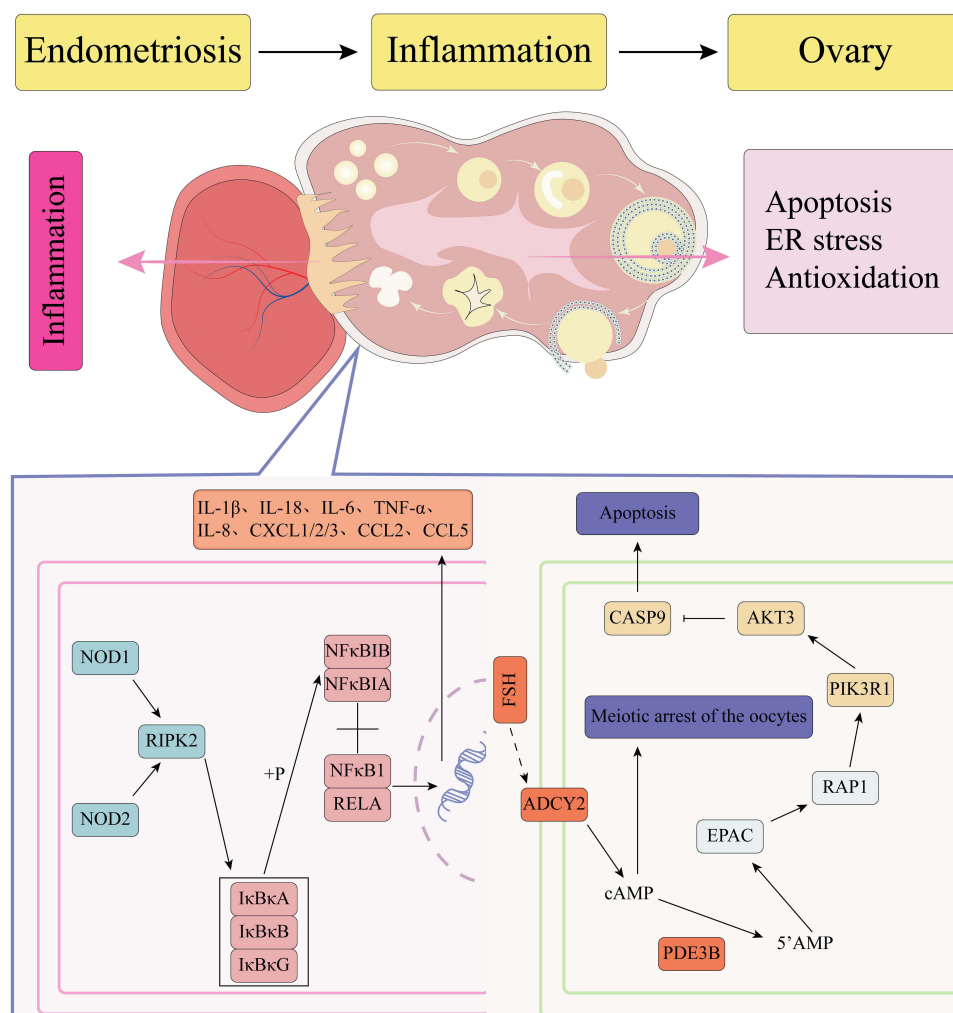


Figure 9 Diagram illustrating the ways via which inflammation caused by endometriotic tissue affects the ovary. The image depicts the process by which ectopic tissue adheres to the ovary and then continuously assaults the ovarian tissue, causing inflammation.

possessed up-regulated targets such as DTL, CPA3, E2F8, and FST, as well as down-regulated targets such as PGR and PNO. XYTJD may correct the aberrant expression of the targets above. Progesterone can stimulate PGR, which in turn causes the endometrium to decidualize. However, PGR expression is decreased in ectopic tissues, leading to decidualization deficiencies in ectopic lesions.²² PNO is a requirement for nociceptin, which belongs to the opioid receptor and possesses analgesic properties.²³ PNO was downregulated in the model's ectopic tissues, which may indicate that PNO is related to dysmenorrhea. Mast cell recruitment and differentiation factor CPA3, which was also found to be increased in our model, can attract mast cells and accelerate the development of inflammation in OEM.²⁴ DTL expression is decreased in human OEM, peritoneal endometriosis, and deep infiltrating endometriosis.²⁵ DTL can control the cell cycle and stimulate tumour growth, invasion, and proliferation.²⁶ The model's ectopic tissues have increased expression, which seems different from that in illness. As a result, additional verification is required on DTL's role in OEM. E2F8 is a transductant of vascular endothelial growth factor, which can bind to blood oxygen inducible factors and enhance vascular endothelial growth factor expression.²⁷ E2F8 expression in ectopic tissues also indicates angiogenesis during the proliferative phase. XYTJD was able to correct the expression of the targets above, implying that it may have the ability to decrease angiogenesis and inflammation and induce decidualization of ectopic tissues in OEM.

Through KEGG enrichment analysis with DEGsAB, the IL-17 signalling pathway in the obtained pathways can activate the pro-inflammatory helper T cell 17, releasing inflammatory components.²⁸ Meanwhile, Th17 is positively associated with the severity of endometriosis.²⁹ According to immune infiltration research, XYTJD enhanced resting

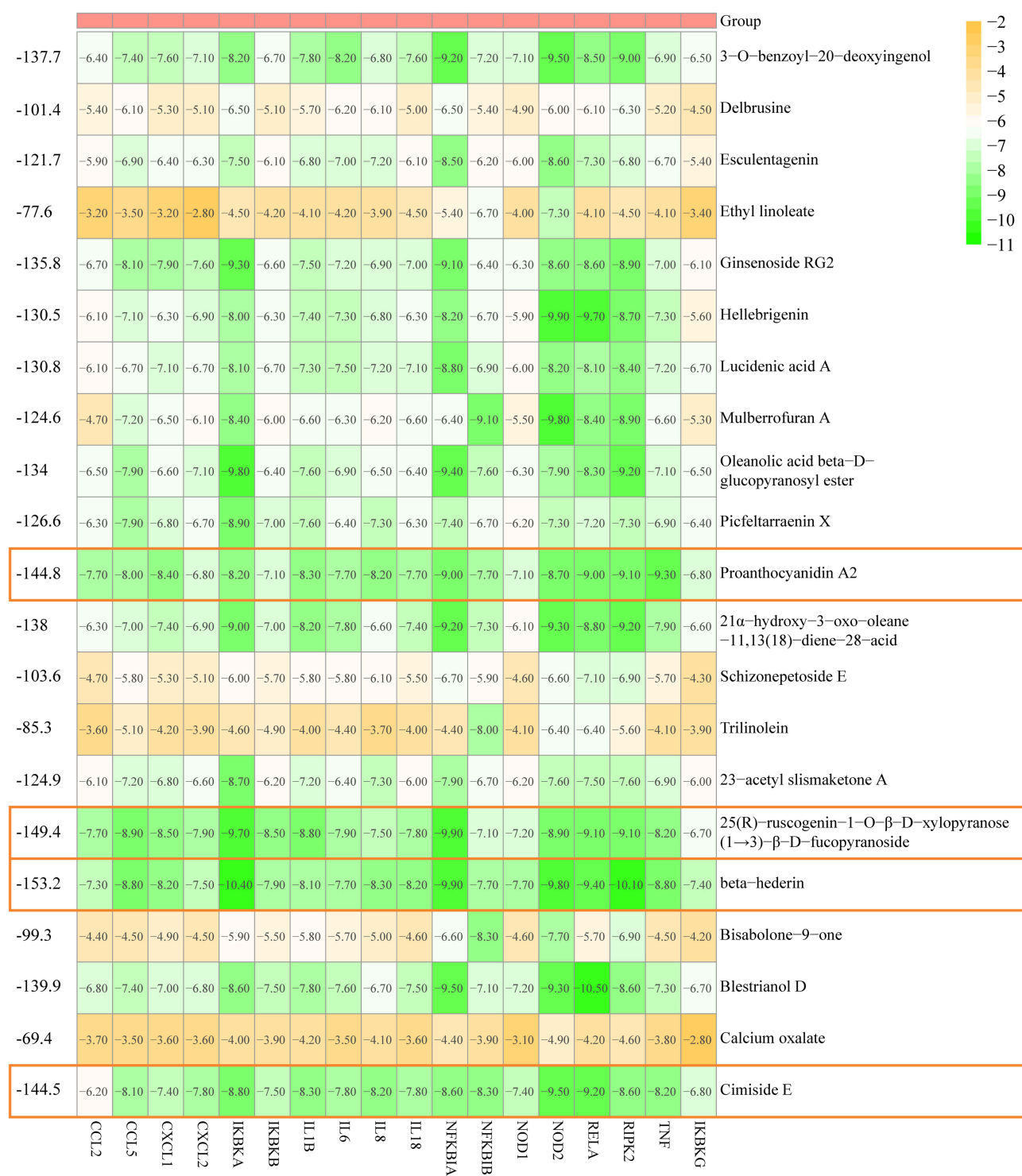


Figure 10 Virtual screening heatmap. The target's name appears at the bottom of the figure. On the left side of the picture is the total energy of binding of a single active ingredient to all targets. The name of the active ingredient is located to the right of the figure shape. The energy of the active ingredient's paired binding to the target site is represented by the little squares in the figure.

dendritic cell clusters in ectopic tissues and decreased follicular helper T and plasma cell clusters. Plasma cells, also known as effector B cells, can produce more immunoglobulin. Significantly more plasma cells are infiltrating the endometriosis patients' eutopic endometrium in endometriosis patients, which may be connected to the aberrant endometrial immune response that lowers endometrial receptivity.³⁰ T follicular helper cells play both protective and

harmful activities, contributing to various immunological disorders and promoting inflammation. However, the impact of T follicular helper cells on OEM lesions is not entirely clear.³¹ Dendritic cells are specialized antigen-presenting cells in the body that can improve angiogenesis and accelerate endometrial development.³² XYTJD may decrease OEM lesions by increasing the number of resting dendritic cells while lowering the number of plasma and follicular helper T cells. Still, the exact mechanism is unknown and requires additional experimental investigation.

The NOD-like receptor, NF κ B, JAK-STAT, TNF, Toll-like receptor, Th1 and Th2 cell differentiation pathways were shown to be considerably higher in ectopic tissues than in normal tissues, according to GSEA enrichment analysis. These pathways are closely associated with the pathogenesis and development of OEM. According to Yeo SG et al,³³ endometriosis patients' peritoneal fluid had much greater levels of NOD1 and NOD2 than normal women. The activation targets of inflammatory disorders include NOD1 and NOD2, and the elevated expression of these receptors in rat ectopic tissues is likewise in line with OEM's characteristics as a chronic inflammatory disease. The NF κ B pathway is the downstream route of both NOD1 and NOD2. One of the well-known pathways in the pathophysiology of OEM is the NF κ B pathway, which controls cell proliferation and inflammation. TNF- α and IL-1 β are two of the downstream factors that can cause inflammation.³⁴ In rat and human ectopic tissues, both the NOD-like receptor and the NF κ B pathways are up-regulated, suggesting that NOD/NF κ B is a significant factor in the inflammation brought on by endometriosis. Important inflammatory factors in endometriosis inflammation include its downstream TNF- α and IL-1 β , and the polymorphisms of these two factors are also endometriosis risk prediction genes.³⁵ In ectopic tissues, XYTJD may dramatically down-regulate the NOD/NF κ B pathway and suppress the expression of TNF- α and IL-1 β , indicating that XYTJD may reduce OEM inflammation through the down-regulation of the NOD/NF κ B system.

The GSEA enrichment analysis of ovarian tissues revealed a considerable down-regulation of the cAMP and PI3K-AKT pathways in ovarian tissues linked to ectopic tissues. The cAMP pathway is involved in oocyte growth and granulosa cell layer production; specifically, cAMP in the path can govern oocyte meiosis arrest.³⁶ The downstream route of cAMP is PI3K-AKT.³⁷ The PI3K-AKT pathway is critical in controlling cell division and preventing apoptosis. It is also a central pathophysiological mechanism in the loss of ovarian function, particularly in the autophagy of granulosa cells.^{38,39} CASP9 is an essential gene that stimulates apoptosis and is a downstream factor of PI3K-AKT. Clinical investigations have also verified the elevated expression of CASP9 in the follicular granulosa cells of individuals with OEM.⁴⁰ Following XYTJD administration, OEM rats showed reduced ectopic tissue inflammation, increased cAMP/PI3K/AKT pathway activity, and decreased CASP9 expression in the ovarian tissues connected to ectopic tissues. These results imply that XYTJD may prevent ovarian cell death by reducing inflammation in OEM ectopic tissues and reestablishing the ovary's downregulated cAMP/PI3K/AKT pathway. Furthermore, we discovered that the ovary with ectopic attachment had significant expression levels of GSTM5 and SEC61B. GSTM5 can accelerate glutathione binding to oxidative agents to shield cells from harm. It also serves as an antioxidant marker.^{41,42} SEC61B plays a critical function in maintaining endoplasmic reticulum homeostasis, and its expression is enhanced when the endoplasmic reticulum is under oxidative stress.⁴³ The increased production of antioxidant factors and inner subnet stress proteins in the ovary linked to ectopic tissue may be an attempt by the ovary to self-regulate in response to ectopic tissue-induced inflammation. Following XYTJD intervention, the expression of GSTM5 and SEC61B in ovarian tissues linked to ectopic tissues reduced, implying that XYTJD may affect ovarian tissues by lowering inflammation in ectopic tissues. Of course, XYTJD may act directly on the ovary, which we must investigate more. According to clinical research, OEM ovarian cells have a lower potential for antioxidants. However, the antioxidant GSTM5 is more expressed in our rat model.⁴⁴ The explanation could be that our model was formed only three weeks after gavage, and ovarian tissue self-regulation has yet to fail.

UPLC-Q-TOF-HRMS detection of drug-containing serum from humans and model rats revealed the presence of 21 active components in both human and rat serum. Several active components with lower energy requirements were found using virtual screening technologies to further batch dock these 21 active components with NOD/NF κ B targets. Examples include 25(R)-ruscogenin-1-O- β -D-xylopyranose(1 \rightarrow 3)- β -D-fucopyranoside, beta-hederin, Cimicide E, and Proanthocyanidin A2. Cimicide E could stop the cell cycle and cause apoptosis in gastric cancer cells.⁴⁵ Furthermore, Cimicide E might possess anti-inflammatory and antioxidant properties.⁴⁶ Proanthocyanidin A2 suppressed the activation of shape cells, implying that it prevented fibrosis.⁴⁷ Many of the active chemicals in this study have not been applied to OEM. Therefore, the involvement of OEM in the active substances requires additional verification by molecular cytology.

This study found that XYTJD may ameliorate ovarian damage by decreasing inflammation in ectopic tissues in OEM during the proliferative phase. The potential mechanism by which XYTJD inhibits inflammation in ectopic tissues is through the downregulation of the NOD/NF κ B pathway. Ectopic tissue-attached ovaries exhibited lower cAMP/PI3K/AKT levels while increasing apoptotic factors, antioxidant proteins, and endoplasmic reticulum stress proteins. However, further research is needed to determine how inflammation influenced these changes in the ovary. In addition, a limitation of this study is that the virtual screening initially revealed the active components in XYTJD, and the individual elements have not yet been tested for their effects in rats.

Abbreviations

NOD1, Nucleotide-binding oligomerization domain-containing protein 1; NOD2, Nucleotide-binding oligomerization domain-containing protein 2; NF κ B, Nuclear factor NF-kappa-B p105 subunit; TNF- α , Tumor necrosis factor; IL-1 β , Interleukin-1 beta; cAMP, Cyclic Adenosine monophosphate; PI3K, phosphatidylinositol 3-kinase; AKT, Serine/threonine protein kinase B; CASP9, Caspase-9; SEC61B, Protein transport protein Sec61 subunit beta; GSTM5, Glutathione S-transferase Mu 5; TGF- β , Transforming growth factor beta-1 proprotein;

JAK, Janus Kinase; STAT, Signal Transducers and Activators of Transcription; ADCY2, Adenylate cyclase type 2; PDE3B, cGMP-inhibited 3',5'-cyclic phosphodiesterase 3B; AKT3, RAC-gamma serine/threonine-protein kinase; PIK3R1, Phosphatidylinositol 3-kinase regulatory subunit alpha; DTL, Denticleless protein homolog; CPA3, Mast cell carboxypeptidase A; E2F8, Transcription factor E2F8; FST, Follistatin; PGR, Progesterone receptor; PNO, Prepronociceptin; IL-17, Interleukin-17; Th17, T helper cell 17; NF κ BIA, NF-kappa-B inhibitor alpha; RIPK2, Receptor-interacting serine/threonine-protein kinase 2; I κ B κ G, NF-kappa-B essential modulator.

Data Sharing Statement

The data analyzed in this study can be obtained from the corresponding author upon reasonable request.

Acknowledgments

Shandong Youth Natural Science Research Project, No. 24ZRK022; The Scientific Planning Academic Project of Youth Education in Shandong Province, No. 24BSH510, No. 23BSH251. Program of TCM Science and Technology in Shandong Province, No. M-2023259.

Author Contributions

All authors made a significant contribution to the work reported, whether that is in the conception, study design, execution, acquisition of data, analysis and interpretation, or in all these areas; took part in drafting, revising or critically reviewing the article; gave final approval of the version to be published; have agreed on the journal to which the article has been submitted; and agree to be accountable for all aspects of the work.

Ethics Approval and Consent to Participate

Animal experiments were approved by the Animal Ethics Committee of Shandong University of Traditional Chinese Medicine (Ethical approval: SDUTCM20231228001), Laboratory animal welfare follows the Replacement, Reduction and Refinement principle. The ethics of human part was approved by the Ethics Committee of the Affiliated Hospital of Shandong University of Traditional Chinese Medicine (Ethics approval: 2023-153-KY). The clinical study complied with the Declaration of Helsinki.

Disclosure

The authors declare that there are no conflicts of interest regarding the publication of this paper.

References

1. Fan W, Yuan Z, Li M, Zhang Y, Nan F. Decreased oocyte quality in patients with endometriosis is closely related to abnormal granulosa cells. *Front Endocrinol.* 2023;14:1226687. doi:10.3389/fendo.2023.1226687

2. Falcone T, Flyckt R. Clinical Management of Endometriosis. *Obstet Gynecol.* 2018;131(3):557–571. doi:10.1097/AOG.0000000000002469
3. Vercellini P, Viganò P, Somigliana E, Fedele L. Endometriosis: pathogenesis and treatment. *Nat Rev Endocrinol.* 2014;10:261–275. doi:10.1038/nrendo.2013.255
4. Koller D, Pathak GA, Wendt FR, et al. Epidemiologic and genetic associations of endometriosis with depression, anxiety, and eating disorders. *JAMA Network Open.* 2023;6:e2251214. doi:10.1001/jamanetworkopen.2022.51214.
5. Busacca M, Vignali M. Ovarian endometriosis: from pathogenesis to surgical treatment. *Curr Opin Obstet Gynecol.* 2003;15(4):321–326. doi:10.1097/01.gco.0000084247.09900.4f
6. Bonavina G, Taylor HS. Endometriosis-associated infertility: from pathophysiology to tailored treatment. *Front Endocrinol.* 2022;13:1020827. doi:10.3389/fendo.2022.1020827
7. Li Y, Li R, Ouyang N, et al. Investigating the impact of local inflammation on granulosa cells and follicular development in women with ovarian endometriosis. *Fertil Steril.* 2019;112(5):882–891.e1. doi:10.1016/j.fertnstert.2019.07.007
8. Fonseca BM, Pinto B, Costa L, Felgueira E, Rebelo I. Increased expression of NLRP3 inflammasome components in granulosa cells and follicular fluid interleukin(IL)-1beta and IL-18 levels in fresh IVF/ICSI cycles in women with endometriosis. *J Assist Reprod Genet.* 2023;40(1):191–199. doi:10.1007/s10815-022-02662-2
9. Orisaka M, Mizutani T, Miyazaki Y, et al. Chronic low-grade inflammation and ovarian dysfunction in women with polycystic ovarian syndrome, endometriosis, and aging. *Front Endocrinol.* 2023;14:1324429. doi:10.3389/fendo.2023.1324429
10. Wei L, Wang J, Zhang Z. Clinical observation of Xuanyu Tongjing decoction and Xuefu Zhuyu capsule in the treatment of endometriosis dysmenorrhea. *Sichuan J Tradit Chin Med.* 2017;35(12):173–175.
11. Zhang X, Huang S, Wang Y. To investigate the effect of modified Xuanyu Tongjing decoction on ovarian function and serum EMB and MMP-9 levels in patients with endometriosis after operation. *Modern J Integr Tradit West Med.* 2021;30:1901–1904.
12. Smith-Unna R, Bournsnel C, Patro R, Hibberd JM, Kelly S. TransRate: reference-free quality assessment of de novo transcriptome assemblies. *Genome Res.* 2016;26(8):1134–1144. doi:10.1101/gr.196469.115
13. Li W, Godzik A. Cd-hit: a fast program for clustering and comparing large sets of protein or nucleotide sequences. *Bioinformatics.* 2006;22(13):1658–1659. doi:10.1093/bioinformatics/btl158
14. Simão FA, Waterhouse RM, Ioannidis P, Kriventseva EV, Zdobnov EM. BUSCO: assessing genome assembly and annotation completeness with single-copy orthologs. *Bioinformatics.* 2015;3:3210–3212. doi:10.1093/bioinformatics/btv351
15. Li B, Dewey CN. RSEM: accurate transcript quantification from RNA-Seq data with or without a reference genome. *BMC Bioinf.* 2011;12:323. doi:10.1186/1471-2105-12-323
16. Conesa A, Madrigal P, Tarazona S, et al. A survey of best practices for RNA-seq data analysis. *Genome Biol.* 2016;17(1):13. Erratum in: *Genome Biol.* 2016;17:181. doi: 10.1186/s13059-016-1047-4. doi:10.1186/s13059-016-0881-8
17. Wang L, Feng Z, Wang X, Wang X, Zhang X. DEGseq: an R package for identifying differentially expressed genes from RNA-seq data. *Bioinformatics.* 2010;26(1):136–138. doi:10.1093/bioinformatics/btp612
18. Fan W, Lei H, Li X, Zhao Y, Zhang Y, Li Y. Exploring the mechanism of yiwei decoction in the intervention of a premature ovarian insufficiency rat based on network pharmacology and the miRNA-mRNA Regulatory Network. *ACS Omega.* 2024;9(17):19009–19019. doi:10.1021/acsomega.3c09551
19. Wei W, Liu S, Han Y, et al. Rapid identification of chemical components in Zhizi Baipi decoction by ultra-performance liquid chromatography quadrupole time-of-flight mass spectrometry coupled with a novel informatics UNIFI platform. *J Sep Sci.* 2022;45(19):3679–3690. doi:10.1002/jssc.202200306
20. Zhang NN, Sun TS, Yang Q. An effective “water injection”-assisted method for excision of ovarian endometrioma by laparoscopy. *Fertil Steril.* 2019;112(3):608–609. doi:10.1016/j.fertnstert.2019.05.014
21. Chauhan JK, Dubey PK, Rai S, Tripathi A. Induction and characterization of a rat model of endometriosis. *Sci Rep.* 2024;14(1):18827. doi:10.1038/s41598-024-69440-1
22. Zhang P, Wang G. Progesterone resistance in endometriosis: current evidence and putative mechanisms. *Int J mol Sci.* 2023;24(8):6992. doi:10.3390/ijms24086992
23. Darland T, Heinricher MM, Grandy DK. Orphanin FQ/nociceptin: a role in pain and analgesia, but so much more. *Trends Neurosci.* 1998;21(5):215–221. doi:10.1016/s0166-2236(97)01204-6
24. Atiakshin D, Patsap O, Kostin A, Mikhalyova L, Buchwalow I, Tiemann M. Mast cell tryptase and carboxypeptidase a3 in the formation of ovarian endometrioid cysts. *Int J mol Sci.* 2023;24(7):6498. doi:10.3390/ijms24076498
25. Jiang L, Zhang M, Wang S, Han Y, Fang X. Common and specific gene signatures among three different endometriosis subtypes. *PeerJ.* 2020;8:e8730. doi:10.7717/peerj.8730
26. Cui H, Wang Q, Lei Z, et al. DTL promotes cancer progression by PDCD4 ubiquitin-dependent degradation. *J Exp Clin Cancer Res.* 2019;38(1):350. doi:10.1186/s13046-019-1358-x
27. Weijts BG, Bakker WJ, Cornelissen PW, et al. E2F7 and E2F8 promote angiogenesis through transcriptional activation of VEGFA in cooperation with HIF1. *EMBO J.* 2012;31(19):3871–3884. doi:10.1038/emboj.2012.231
28. He Y, Yang Q, Zhang T, et al. Pathogenic characteristics of Th17 cells based on the IL-17 signaling pathway in the regulation of sebaceous gland lipoprotein metabolism in an acne rat model. *Iran J Immunol.* 2021;18(3):203–209. doi:10.22034/iji.2021.88231.1855
29. Gogacz M, Winkler I, Bojarska-Junak A, et al. Increased percentage of Th17 cells in peritoneal fluid is associated with severity of endometriosis. *J Reprod Immunol.* 2016;117:39–44. doi:10.1016/j.jri.2016.04.289
30. Freitag N, Baston-Buest DM, Kruessel JS, Markert UR, Fehm TN, Bielfeld AP. Eutopic endometrial immune profile of infertility-patients with and without endometriosis. *J Reprod Immunol.* 2022;150:103489. doi:10.1016/j.jri.2022.103489
31. Dong L, He Y, Cao Y, et al. Functional differentiation and regulation of follicular T helper cells in inflammation and autoimmunity. *Immunology.* 2021;163(1):19–32. doi:10.1111/imm.13282
32. Pencovich N, Luk J, Hantisteanu S, Hornstein MD, Fainaru O. The development of endometriosis in a murine model is dependent on the presence of dendritic cells. *Reprod Biomed Online.* 2014;28(4):515–521. doi:10.1016/j.rbmo.2013.12.011
33. Yeo SG, Won YS, Lee HY, Kim YI, Lee JW, Park DC. Increased expression of pattern recognition receptors and nitric oxide synthase in patients with endometriosis. *Int J Med Sci.* 2013;10(9):1199–1208. doi:10.7150/ijms.5169

34. Ponce C, Torres M, Galleguillos C, et al. Nuclear factor kappaB pathway and interleukin-6 are affected in eutopic endometrium of women with endometriosis. *Reproduction*. 2009;137(4):727–737. doi:10.1530/REP-08-0407
35. Mier-Cabrera J, Cruz-Orozco O, de la Jara-Díaz J, et al. Polymorphisms of TNF-alpha (-308), IL-1beta (+3954) and IL1-Ra (VNTR) are associated to severe stage of endometriosis in Mexican women: a case control study. *BMC Women's Health*. 2022;22(1):356. doi:10.1186/s12905-022-01941-5
36. Johnson AL. Ovarian follicle selection and granulosa cell differentiation. *Poult Sci*. 2015;94(4):781–785. doi:10.3382/ps/peu008
37. Baviera AM, Zanon NM, Navegantes LC, Kettelhut IC. Involvement of cAMP/Epac/PI3K-dependent pathway in the antiproteolytic effect of epinephrine on rat skeletal muscle. *mol Cell Endocrinol*. 2010;315(1–2):104–112. doi:10.1016/j.mce.2009.09.028
38. Liu S, Jia Y, Meng S, Luo Y, Yang Q, Pan Z. Mechanisms of and potential medications for oxidative stress in ovarian granulosa cells: a review. *Int J mol Sci*. 2023;24(11):9205. doi:10.3390/ijms24119205
39. Hu W, Xie N, Pan M, et al. Chinese herbal medicine alleviates autophagy and apoptosis in ovarian granulosa cells induced by testosterone through PI3K/AKT1/FOXO1 pathway. *J Ethnopharmacol*. 2024;318:117025. doi:10.1016/j.jep.2023.117025
40. Chen L, Ni Z, Cai Z, et al. The mechanism exploration of follicular fluids on granulosa cell apoptosis in endometriosis-associated infertility. *Biomed Res Int*. 2021;2021:6464686. doi:10.1155/2021/6464686
41. Jin DX, Jia CY, Yang B, et al. The ameliorative mechanism of *Lactiplantibacillus plantarum* NJAU-01 against d-galactose induced oxidative stress: a hepatic proteomics and gut microbiota analysis. *Food Funct*. 2024;15(11):6174–6188. doi:10.1039/d4fo00406j
42. Song G, Nesil T, Cao J, Yang Z, Chang SL, Li MD. Nicotine mediates expression of genes related to antioxidant capacity and oxidative stress response in HIV-1 transgenic rat brain. *J Neurovirol*. 2016;22(1):114–124. doi:10.1007/s13365-015-0375-6
43. Tomiyama R, Takakura K, Takatou S, et al. 3,4-dihydroxybenzalacetone and caffeic acid phenethyl ester induce preconditioning ER stress and autophagy in SH-SY5Y cells. *J Cell Physiol*. 2018;233(2):1671–1684. doi:10.1002/jcp.26080
44. Da Broi MG, de Albuquerque FO, de Andrade AZ, Cardoso RL, Jordão Junior AA, Navarro PA. Increased concentration of 8-hydroxy-2'-deoxyguanosine in follicular fluid of infertile women with endometriosis. *Cell Tissue Res*. 2016;366(1):231–242. doi:10.1007/s00441-016-2428-4
45. Guo LY, Joo EJ, Son KH, et al. Cimicid E arrests cell cycle and induces cell apoptosis in gastric cancer cells. *Arch Pharm Res*. 2009;32(10):1385–1392. doi:10.1007/s12272-009-2007-2
46. Moon L, Ha YM, Jang HJ, et al. Isoimperatorin, cimicid E and 23-O-acetylshengmanol-3-xyloside from *Cimicifugae* rhizome inhibit TNF- α -induced VCAM-1 expression in human endothelial cells: involvement of PPAR- γ upregulation and PI3K, ERK1/2, and PKC signal pathways. *J Ethnopharmacol*. 2011;133(2):336–344. doi:10.1016/j.jep.2010.10.004
47. Xiao Y, Li X, Wang L, Hu M, Liu Y. Proanthocyanidin A2 attenuates the activation of hepatic stellate cells by activating the PPAR- γ signalling pathway. *Autoimmunity*. 2023;56(1):2250101. doi:10.1080/08916934.2023.2250101

Drug Design, Development and Therapy

Publish your work in this journal

Drug Design, Development and Therapy is an international, peer-reviewed open-access journal that spans the spectrum of drug design and development through to clinical applications. Clinical outcomes, patient safety, and programs for the development and effective, safe, and sustained use of medicines are a feature of the journal, which has also been accepted for indexing on PubMed Central. The manuscript management system is completely online and includes a very quick and fair peer-review system, which is all easy to use. Visit <http://www.dovepress.com/testimonials.php> to read real quotes from published authors.

Submit your manuscript here: <https://www.dovepress.com/drug-design-development-and-therapy-journal>

Dovepress
Taylor & Francis Group